Z. Kristallogr. **2013**, *228*, 607–610 / **DOI** 10.1524/zkri.2013.1654

Symmetry and the polar state of condensed molecular matter

Jürg Hulliger*, Thomas Wüst, and Mathias Rech

Department of Chemistry and Biochemistry, University of Berne, Freiestr. 3, 3012 Bern, Switzerland

Received May 2, 2013; accepted August 18, 2013
Published online: December 5, 2013

Bi-polar state / Condensed molecular matter / Electrical polarization / Monte Carlo simulation / Thermal equilibrium / Symmetry

Abstract. Polar molecular crystals seem to contradict a quantum mechanical statement, according to which no stationary state of a system features a permanent electrical polarization. By stationary we understand here an ensemble for which thermal averaging applies. In the language of statistical mechanics we have thus to ask for the thermal expectation value of the polarization in molecular crystals. Nucleation aggregates and growing crystal surfaces can provide a single degree of freedom for polar molecules required to average the polarization. By means of group theoretical reasoning and Monte Carlo simulations we show that such systems thermalize into a bi-polar state featuring zero bulk polarity. A two domain, *i.e.* bi-polar state is obtained because boundaries are setting up opposing effective electrical fields. Described phenomena can be understood as a process of partial ergodicity-restoring. Experimentally, a bi-polar state of molecular crystals was demonstrated using phase sensitive second harmonic generation and scanning pyroelectric microscopy.

" ... I was just taught that nothing has an electric dipole moment."

P. W. Anderson[1]

Contrary to P. W. Anderson, most of us were taught that asymmetrical molecules feature a permanent electric dipole moment: Quantum chemistry is showing that the most probable nuclear configuration for, say, two hydrogen atoms and one oxygen is the structure of water representing *mm*2 symmetry. This means, on the level of most single molecules we are allowed to assume a permanent electric dipole moment. However, the quantities to be measured for an ensemble of molecules are thermal expectation values ($\langle P_{vol}\rangle$; *P*: polarization). In this respect, the teacher of Anderson was careful enough to say "... that no stationary state of a system ... has an electric dipole moment" [1].

The underlying question suggested by our title is: *Can a condensed state of molecular matter yield a thermal expectation value for* $\langle P_{vol}\rangle$ *different from zero?*

A droplet of pure water in the absence of an electrical field may serve as an introductory example. Here, dipole moments μ_{el} follow an angular distribution yielding $\langle P_{vol}\rangle = 0$, *i.e.* the symmetry of the degrees of freedom to randomize the vector property is spherical $(\infty/m\ \infty/m\ \infty/m)^2$. So far, we were not taking into account that any finite system encounters boundaries, where symmetry breaking takes place: At the droplet's surface complete randomness of the polarization gets lost and thus the boundary is charged by polarized water molecules [3].

Now, assuming dipole moments of molecules within a crystal, these vectors can be projected onto an axis, running through a lattice. For reasons of symmetry, this projection may yield non-zero values only for the pyroelectric point groups [4]. Given the axis, the one dimensional space for thermal averaging represents symmetry ∞/m. Because of a finite size effect ∞/m reduces to $\infty/\infty m$ [2] (see Schema 1), *i.e.* a bi-polar state allowing for polar properties of symmetry ∞/m (μ_{el}, *P*) in each domain.

An adequate frame to analyse crystal polarity is the Ising model [5]. Contrary to the case of magnetism, for asymmetrical (polar) molecules A–D (A: acceptor frame; D: donor frame; μ_{el} pointing from A to D) at least three effective energy parameters are necessary to account for nearest neighbour contacts (···): Two *longitudinal* $\Delta E_A = E_{AA} - E_{AD}$, $\Delta E_D = E_{DD} - E_{AD}$ (where E_{AD}: A–D ··· A–D; E_{AA}: D–

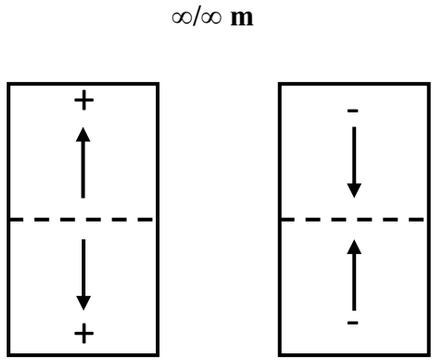

Bi-polar macrostates of solid matter

Schema 1. A schematic representation of bi-polar states [2]: The object is built of two domains of opposite polarities, yielding zero in total. $\infty/\infty m$: Symbol of the corresponding continuous group.

* Correspondence author (e-mail: juerg.hulliger@iac.unibe.ch)

A $\cdots$ A–D; E_{DD}: A–D $\cdots$ D–A) parameters and one *lateral* energy difference $\Delta E_\perp = E_p - E_{ap}$ (p: parallel alignment; ap: antiparallel alignment).

So, for the purpose of calculation, molecules are replaced by vectors to undergo tip-tip, back-back and tip-back interactions. A real representation may be given by prolate type molecules carrying A and D substituents at either end, respectively (A, D substituted phenyl, bi-phenyl, stibenes).

An instructive configuration of molecules to study the thermal average of P is a *finite linear chain*. The Hamiltonian [6] of the system (Eq. (1)) contains two linear terms of opposite signs accounting for molecules located at each end of the chain (boundaries at 0 and L; see Fig. 1). These contributions feature electric E-field character $(\infty/m)^2$, although there is no external field applied. Such surface terms only exist for intermolecular interactions providing that E_{AA} is different from E_{DD}:

$$H_{chain} = \varepsilon + {}^1\!/_4 \{S_0\,\Delta E_f - S_L\,\Delta E_f - (\Delta E_A + \Delta E_D)\,\Sigma S_i S_{i+1}\} \quad (i = 0, \ldots, L-1), \qquad (1)$$

where $\Delta E_f = \Delta E_A - \Delta E_D = E_{AA} - E_{DD}$; ϵ: constant; S: effective particle operator.

Estimating $\langle P_{chain}\rangle$ numerically by Monte Carlo simulations [7], we find regions of *opposite* polarities near either end (Fig. 1). Obviously, the total polarization $\langle P_{chain}\rangle$ is zero. The sign of the surface charge at boundaries 0 and L is given by ΔE_f: For $\Delta E_f > 0$, acceptor parts A (negative charge) preferably appear at both ends.

Next we consider a model for a *seed crystal*, having emerged from the process of homogeneous nucleation. Here, we introduce coupling to four neighbours in the lateral direction ($\Delta E_\perp$) and to two neighbours in the direction of the polar axis (ΔE_A, ΔE_D). Again the Hamiltonian $H_{crystal}$ contains surface related terms of opposite signs, acting as E-fields. Monte Carlo simulations revealed a similar general behaviour as found for the 1D system, representing a bi-polar state (see Fig 2). Here, the lateral interaction ($\Delta E_\perp$) favouring parallel alignment is strongly influencing the total extent of polarity and its spatial distribution.

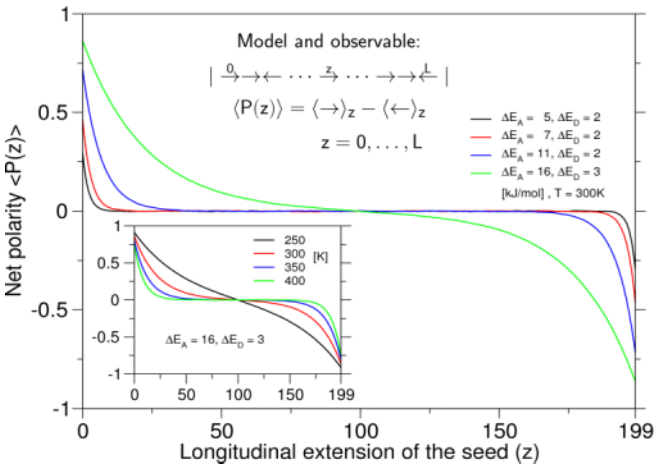

Fig. 1. Polarity formation within a finite chain of nearest neighbour coupled molecules A–D meeting boundaries at 0 and L. The chain is set to thermal equilibrium with respect to dipole reversal (180°), calculated by Monte Carlo simulations. $\langle P(z)\rangle$: Thermal average polarization at position z of the chain. Domains of opposite polarities appear near boundaries. Inset: Temperature dependence of $\langle P(z)\rangle$.

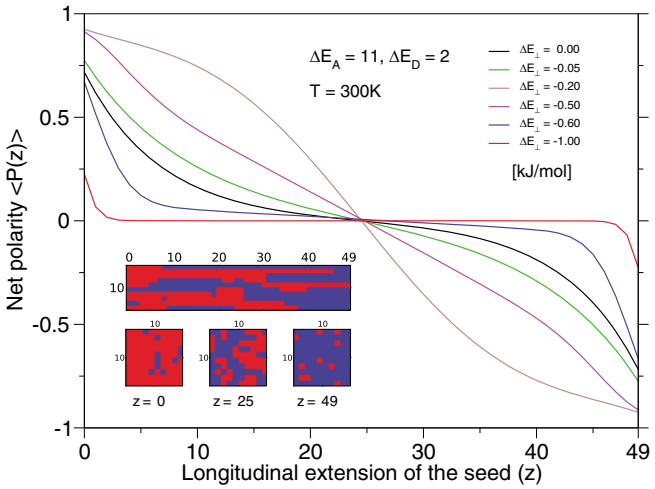

Fig. 2. Net polarity for a nano-sized seed crystal (3D: $10 \times 10 \times 50$ molecules) made of molecules A–D, obtained from Monte Carlo simulations. $\langle P(z)\rangle$: Thermal expectation value of the polarization. Perpendicular to the polar axis of alignment periodic boundary conditions were applied. Starting from a state of random orientation, thermalization is leading to a *bi-polar* state featuring $\langle P_{vol}\rangle = 0$. Insets: Snap shots of the state of alignment along the axis (above) and perpendicular to it (below). Blue and red colours symbolize opposite dipole orientations.

In case Monte Carlo calculation for the 1D and 3D case would be performed for a size much larger than the nano region, bi-polarity is found only as a surface near effect.

Following a concept introduced by P. Curie [8], the symmetry group ∞ of a polar surface-near *domain* is obtained by the symmetry breaking effect of the field terms (∞m) in H acting on the space of the degree of freedom (∞/m) for reversal of a vector property: $\infty = \infty m \cap \infty/m$. As these fields appearing in the Hamiltonian H carry opposite signs, we can argue in the following way: Domain with boundary 0: $\infty m \cap \infty/m = \infty$; domain with boundary L (see Fig 1): $-\infty m \cap \infty/m = -\infty$; yielding $\langle P_0\rangle + \langle P_L\rangle = 0$. According to Shubnikov *et al.* [2], the symmetry group of the entire system is $\infty/\infty m$, *i.e.* a *bi-polar state* (Schema 1).

The result gained by group theory allows us to conclude: The stationary state of an as nucleated seed crystal is bi-polar ($\infty/\infty m$), the total polarization being zero.

To understand the *growth* of a crystal after nucleation has occurred we consider dipole reversal taking place only at the surface of a growing seed. For that purpose we have investigated a layer-by-layer growth model [9] describing effects of polarity. In such a case also a *bi-polar* state is obtained. The layer-by-layer growth model undergoes a peculiar dynamic transition for a *uni-domain polar* seed at the origin (see Fig. 3): Along one orientation of the polar axis only a few defects exist (blue part), whereas in the counter orientation the system undergoes complete dipole reversal (red part), which can start from a *single* defect. The sign of ΔE_f (Eq. (1)) is determining which orientation will undergo global reversal.

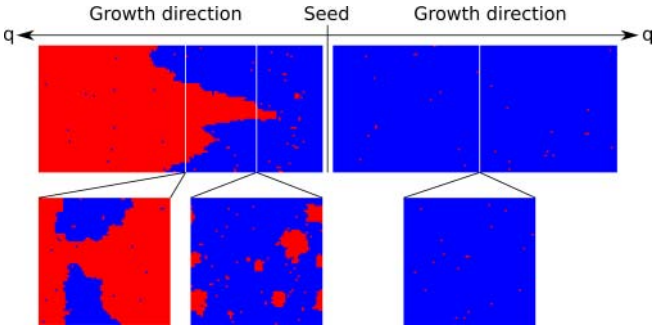

Fig. 3. Monte Carlo simulations for the layer-by-layer growth model demonstrating stochastic dipole reversal when starting with a *uni-domain polar* seed. *Above*: Cross-section parallel to the polar axis. *q*: Number of attached layers along both orientations. Upon a low density of reverted entities cone-shaped structures suddenly can evolve, leading to global reversal after a sufficient number *q* of attached layers along only *one* growth direction (left side). For the opposite direction of growth (right side), no evidence for global reversal was found. *Below*: Cross-sections taken perpendicular to the growth direction show the beginning of several cone-like structures leading to global reversal. Lattice size 64×64 molecules; periodic boundaries in lateral directions. $\Delta E_A = 5$, $\Delta E_D = 2$, $\Delta E_\perp = -2.4$ [kJ/mol], $T = 300$ K.

Summarizing theoretical results on crystals emerging from (i) nucleation or (ii) growth, we are about to extend our conclusion given above:

Irrespective of a process such as nucleation or growth, the stationary polar state of a crystal built from asymmetric molecules A–D populating a degree of freedom ∞/m is expected to show a bi-polar symmetry ∞/∞m and a total polarization $\langle P_{vol} \rangle$ equal to zero.

Basic findings concerning a *bi-polar* state are experimentally well confirmed [10] for as grown crystals involving (i) channel-type inclusion compounds [11], (ii) single component molecular crystals [12], (iii) solid solutions of molecular crystals [13], (iv) dye stained inorganic host lattices [14], (v) some ionic crystals [10] and (vi) even natural tissues [15, 16]. Particularly instructive are (i) channel type inclusion compounds and (ii) single component molecular crystals, nucleating both into a *centric* seed, but developing a *bi-polar* state during growth. Just recentely, experimental evidence for dipole reversal in 4-iodo-4'-nitrobiphenyl, a polar crystal (mm2), was found by scanning pyroelectric microscoppy [17].

In view of these examples confirming bi-polarity, we have now to provide a reason for the appearance of many molecular crystals [18] featuring a *polar* morphology and structure: Typically, nucleation takes place at a higher driving force than growth. Therefore, kinetic effects may lead either to a (i) bi-polar or a (ii) uni-domain polar seed, developing further into a (i) classical twin or (ii) uni-domain polar crystal undergoing reversal, respectively. However, the stochastic demand for an increasing number of faulted orientations emerging around a single defect in case of reversal (Fig. 3, left part) may accumulate critical stress along non-crystallographic, *i.e.* random twin boundaries resulting in a slowing down or complete stop of growth. It is an experimental fact that polar morphologies can show a pronounced growth speed anisotropy [19]. A possible mechanism leading to uni-domain polar molecular crystals is thus *kinetic control* for reasons of stochastic formation of orientational defects.

It is a statistical fact that $P2_1/c$ is the most frequently occurring space group for molecular crystals [18, 20]. The corresponding point group 2/*m*, a subgroup of ∞/*m*, is allowing for a single degree of freedom with respect to reversal. In some of these structures dipolar molecules ideally show a site population of 50 : 50% for either orientation, in others there are anti-parallel chains. This large class of compounds allows us to perform an experimentum crucis: Both scanning pyroelectric and scanning piezoelectric [21] microscopy can distinguish between (i) a as grown bi-polar state to be found within sectors involving the *k* index of (*hkl*) faces, and (ii) an effect of bulk thermalization leading to surface near bi-polarity along the twofold axis, not being bound to particular growth sectors (Schema 2). Similar effects may occur for other point groups. A symmetry analysis for all 32 point groups taking into account prominent (*hkl*) faces is published in Ref. [22].

We started our discussion with the example of a water droplet. Projecting $\langle \mu_{el} \rangle$ of H_2O molecules onto an axis running through the centre of a droplet, we can say that thermal averaging near the surface preserves some polarity because of Eq. (1) and results of Fig. 1. In case the oxygen O ··· O repulsion on average is more effective than that of 2 H ··· H2, ΔE_f is greater than zero and consequently acceptor moieties (O) preferably will cover the surface, carrying a negative charge. Recently, a comprehensive review has reported a negative surface charge for water [3].

Preliminary experiments investigating droplets of aceton, 2-butanon and others solvents by a second harmonic experiment ($\omega_0 = 1064$ nm) revealed polar effects in droplets in the size range of 10–30 micrometer.

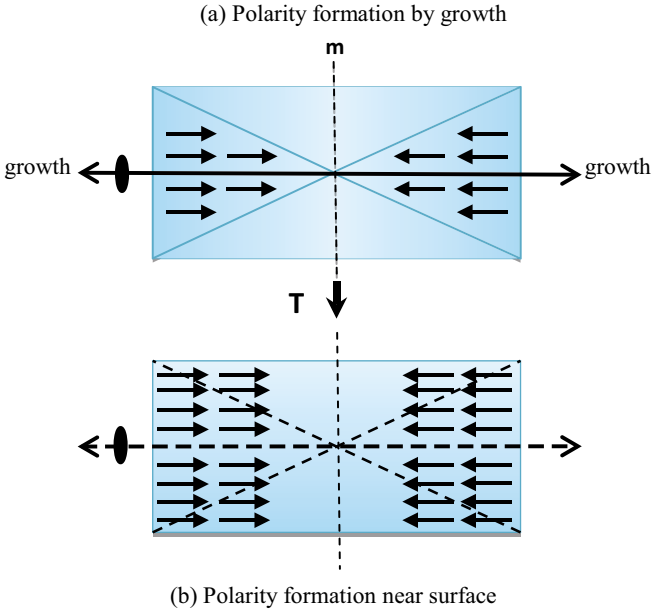

Schema 2. Schematic view featuring two different bi-polar states of a possible crystal with symmetry 2/*m*. In (**a**) the attachment process during growth of a centric seed is responsible for polar alignment in sectors (blue), whereas in (**b**) bulk (blue) thermalization is active. A crystal of point group 2/*m* grown at low temperature may by annealing close to the temperature (T) transform from the (**a**) into the (**b**) state. In the centric seeding state, here for simplicity the molecules axes are assumed to be aligned parallel to the twofold axis. In case of a macroscopic size (**b**) polarity will be reduced to a surface near effect.

Our analysis presents an example for a general behaviour of nature: In case there is local symmetry breaking (here: boundaries 0, L), the system will react to preserve symmetry at the macroscopic level. For polar molecular crystals, the system gets partitioned into at least two corresponding domains (Schema 1, Figs. 2, 3) featuring opposite polarities. In related fields, this behaviour is described by processes of ergodicity-restoring [23].

Technical details on MC simulations

The results of Schem. 1, Fig. 1 (thermodynamic average of $\langle P(z) \rangle$) have been obtained by means of Metropolis sampling using single-spin-flip dynamics [7]. Starting from a random initial state, about 10^6 lattice sweeps were performed to bring a system into equilibrium. $P(z)$ was measured every 10^3 lattice sweeps accumulating a total of about 10^4 measurements. Finally, $\langle P(z) \rangle$ is obtained as the average of at least 10 independent MC simulations. For most energy parameters the results showed negligible statistical errors. Only for strong lateral coupling ($\Delta E_{\perp} < -0.6$ kJ/mol, Fig. 1) errors became noticeable. However, these fluctuations do not alter the significance of $\langle P(z) \rangle$ curves. For more details on the MC procedure, see ref. [9].

Acknowledgements. We would like to thank a number of colleagues for their critical reading and helpful comments. This work was supported by the SNF, project no. 200021_129472/1.

References

[1] Anderson, P. W.: More is different. Science. **177** (1972) 393–396.
[2] Shubnikov, A. V.; Zheludev, I. S.; Konstantinova, V. P.; Silvestrova, I. M.: Investigations of Piezoelectric Textures. Sov. Acad. Sci. Press, Moscow 1955.
[3] Chaplin, M.: Theory *vs.* experiment: What is the surface charge of water*?* Water. **1** (2009) 1–28.
[4] Nye, J. F.: Physical Properties of Crystals. Clarendon Press, Oxford 1985.
[5] Plischke, M.; Bergersen, B.: Equlilibrium Statistical Physics. World Scientific, Singapore 2006.
[6] Bebie, H.; Hulliger, J.: Thermal equilibrium polarization: a near-surface effect in dipolar-based molecular crystals. Physica A. **278** (2000) 327–336.
[7] Binder K.; Heermann, D. W.: Monte Carlo Simulation in Statistical Physics, Springer, Berlin 1997.
[8] Curie, P.: Lois expérimentales du magnétisme. Propriétés magnétiques des corps à diverses températures. J. Phys. **3** (1894) 393–416.
[9] Bebie, H.; Hulliger, J.; Eugster, S.; Alaga-Bogdanovic, M.: Ising model of polarity formation in molecular crystals: from the growth model to the asymptotic equilibrium state. Phys. Rev. **E66** (2002) 021605.
[10] Hulliger, J.; Wüst, T.; Brahimi, K.; Burgener, M.; Aboulfadl, H.: A stochastic principle behind polar properties of condensed molecular matter. New J. Chem. **37** (2013) 2229–2235.
[11] Quintel, A.; Hulliger, J.; Wübbenhorst, M.: Analysis of the Polarization Distribution in a Polar Perhydrotriphenylene Inclusion Compound by Scanning Pyroelectric Microscopy. J. Phys. Chem. **B 102** (1998) 4277–4283 .
[12] Behrnd, N.-R.; Couderc, G.; Wübbenhorst, M.; Hulliger, J.: Scanning pyroelectric microscopy revealing the spatial polarity distribution in topologically centric crystals of trans-4-chloro-4'-nitrostilbene. PCCP. **8** (2006) 4132–4137.
[13] Kluge, S.; Dohnke, I.; Budde, F.; Hulliger, J.: Polarity formation in solid solutions: (4,4′-dinitrostilbene)$_{1-x}$ – (4-chloro-4'-nitrostilbene)$_x$, $1 > x > 0$. CrystEngCom, **5** (2003) 67–69.
[14] Aboulfadl, H.; Burgener, M.; Benedict, J.; Kahr, B.; Hulliger, J.: Polar alignment of dye molecules in sectors of host lattices revealed by phase sensitive second harmonic generation and scanning pyroelectric microscopy. CrystEngCom. **14** (2012) 4391–4395.
[15] Athenstaedt, H.: Permanent longitudinal electric polarization and pyroelectric behaviour of collagenous structures and nervous tissue in man and other vertebrates. Nature. **228** (1970) 830–834.
[16] Hulliger, J.: Connective tissue polarity unraveled by a markov-chain mechanism of collagen fibril segment self-assembly. Biophys. J. **84** (2003) 3501–3507.
[17] Burgener, M.; Labat, G.; Bonin, M.; Morelli, A.; Hulliger, J.: Pyroelectric and piezoelectric scanning microscopy applied to reveal the bipolar state of 4-iodo-4′-nitrobiphenyl (INBP). CrystEngComm. **15** (2013) 7625–7834.
[18] Allen, F. H.: The Cambridge Structural Database: a quarter of a million crystal structures and rising. Acta Cryst. **B58** (2002) 380–388.
[19] Curtin, D. Y.; Paul, I.: Chemical consequences of the polar axis in organic solid-state chemistry. Chem. Rev. **81** (1981) 525–541.
[20] Kitaigorodsky, A. I.: Mixed Crystals (Solid-State Sciences 33), Springer, Berlin 1984.
[21] Batagiannis, A.; Wübbenhorst, M.; Hulliger, J.: Piezo- and pyroelectric microscopy. Curr. Opin. Solid State Mater. Sci. **14** (2010) 107–115.
[22] Gervais, C.; Hulliger, J.: Impact of surface symmetry on growth-induced properties. Cryst. Growth Des. **7** (2007) 1925–1935.
[23] Sethna, J. P.: Statistical Mechanics: Entropy, Order Parameters and Complexity, Oxford university press, Oxford 2006.